Acta Physica Academiae Scientiarum Hungaricae, Tomus 49 (1—3), pp. 39—53 (1980)

X-RAYS INDUCED BY LIGHT IONS

By

H. PAUL

INSTITUTE FOR PHYSICS, JOHANNES KEPLER UNIVERSITY
LINZ, A-4040 LINZ/AUHOF, AUSTRIA

The main processes involved in energy loss of charged particles are briefly considered and compared to inner shell ionization. Some applications of particle induced X-ray emission are mentioned. The higher order corrections to the PWBA and SCA theories for the ionization cross section are briefly sketched and compared to each other.

Selected K-shell cross section data (from the compilation by GARDNER and GRAY, and from some recent publications) for projectiles from protons to oxygen ions on various targets are compared to each other and to theories. It is found that almost all the data lie between 60% above and 60% below the corrected PWBA theory by BRANDT et al, but that there are also systematic discrepancies between theory and experiments where the reduced velocity variable ξ has about the values 0.2, 0.3, and 0.6. Possible reasons for these discrepancies are given. The SCA theory, as corrected by LAEGSGAARD et al, has a rather limited range of validity, but within this range, it agrees better with the data than the PWBA theory.

1. Introduction

It may be useful first to consider what happens to a beam of light ions (e. g. 1 MeV protons) as it hits a solid. Let us assume that there will be about 1 ionizing collision per atomic target layer and that each ionizing collision produces, as in a gas, an energy loss of about 30 eV. Then we expect a range of about 3×10^4 atomic layers or 6μm (assuming an average layer spacing of 0.2 nm, as for Cu). Indeed, the range of 1 MeV protons in Cu is 7 μm [1]. It follows that 1 MeV protons are useful to investigate thin films or near-surface layers.

Actually, the stopping is not constant as we have assumed but reaches a maximum at about 100 keV [1]. At this energy, the proton velocity is just twice the Bohr velocity, v_0. Hence it seems plausible that the stopping power has its maximum where the proton velocity is close to the orbital velocity of outer target electrons.

Compared to those ionizing collisions which affect mainly the outermost electrons, K-shell ionization is a very rare process. Indeed, since the K-shell ionization cross section for 1 MeV protons on Cu is 17b, the probability to produce 1 K-shell hole throughout the range, given by the cross section times the number of target atoms per unit surface, is less than 10^{-3}. Nevertheless this process is easily detected via the subsequent X-radiation.

In analogy to the stopping power, we may expect the maximum K-shell ionization where the projectile velocity v_1 matches the orbital velocity of target K-shell electrons, v_{2K}, To express this expectation also in terms of energy, we introduce the variable η_K [2]:

$$\eta_K = \frac{v_1^2}{v_{2K}^2} = \frac{m}{M_1} \cdot \frac{E_1}{Z_{2K}^2 R} = \frac{\Theta_K}{4} \frac{T_m}{I_K}, \tag{1}$$

where $Z_{2K} = Z_2 - 0.3$ corrects for inner shielding, Θ_K ($0.6 \lesssim \Theta_K \lesssim 1$) for outer shielding. $R = 13.6$ eV is the Rydberg energy, $T_m = 4mE_1/M_1$ is the maximum possible energy transfer to a free electron (mass m) at rest, E_1 is the incident projectile energy, M_1 the projectile mass, I_K the experimental K-ionization energy. The indices 1 and 2 refer to projectile and target, respectively.

In these terms, the maximum cross section is expected where $\eta_K \approx 1$ or where $T_m \approx 4I_K$. On the other hand, a collision with an electron which is free except that its binding energy must be overcome, could never lead to ionization if $T_m < I_K$. Or conversely, it is only the binding that makes ionizing collisions in the low energy region possible [2]. Hence we expect the low energy cross section to increase strongly with increasing η_K and to decrease strongly with increasing Z_2. This behaviour of the cross section is clearly seen, e. g. in the figures given by BASBAS et al [3].

2. Applications

The measurement of particle induced X-ray emission (PIXE) is well suited to determine the concentration of many elements simultaneously in small samples, with ppm sensitivity. Many applications have been described in the first conference on this subject [4], and more recently in [5].

PIXE measurements may also be used to determine the depth profile of a foreign element in bulk material, due to the strong variation of the cross section with energy. If one assumes, e. g., that the foreign atoms occupy a layer of thickness b at a mean depth a, with a concentration c, then these three parameters may be determined by measuring the X-ray yield of the sample at three different energies, if the yield for a thick layer of the pure foreign material is also known [6]. This method, although not as generally applicable as Rutherford backscattering, should be useful for elements of similar Z, for low-Z foreign material in high-Z bulk, and for foreign material of low concentration. Another recent application of this method has been published by VEGH et al [7].

3. Theoretical description

Clearly, the quantitative application of PIXE requires either calibration measurements on known samples, or a knowledge of the cross sections. Empirical relations could be used here [8], but it is also of interest to see how well the cross sections are described by theoretical approaches. In the following, we restrict the discussion to K-shell ionization by light ions ($Z_1 < 0.3\, Z_2$).

Two basic approaches have recently been used with considerable success: the semi-classical approximation (SCA) [9] and the Plane-Wave-Born-Approximation (PWBA) [2]. It has been shown that both approaches must lead to identical results if the same electron wave functions are used [10]. The SCA approach can be easily visualized: the projectile passes the target atom at a distance b from the nucleus, flying in a straight line at constant speed, and it ionizes the K-shell through its rapidly varying electric field. Integrating over all impact parameters b yields the total cross section, σ_K.

Both approaches correspond to first order perturbation; the cross section obtained is therefore proportional to Z_1^2 and depends on the projectile energy only through v_1 [11].

It is useful to know which impact parameter b contributes most to the total σ_K, for a given v_1. Here again, the simplest classical argument leads to a correct result: the collision time (of the oder b/v_1) should be comparable to the period of revolution, $1/\omega_K$. Hence the largest contribution comes from $b = v_1/\omega_K = r_{ad}$, where r_{ad} is the so-called "adiabatic distance" [9]:

$$r_{ad} = v_1/\omega_K = \hbar v_1/I_K \,. \tag{2}$$

In terms of r_{ad}, we may define a reduced velocity ξ which bears a simple relation to η_K:

$$\xi = r_{ad}/a_{2K} = (2/\Theta_K)\sqrt{\eta_K}\,, \tag{3}$$

where $a_{2K} = a_0/Z_{2K}$ is the screened hydrogenic K-shell radius. When properly normalized, σ_K is a universal function of ξ [3]. Although the basic features of the cross section are well described by both theories, a detailed comparison with experiments shows the necessity of additional corrections:

a. Increased binding. At low v_1, where $\xi \ll 1$, the projectile passes well within the target K-shell radius, thus increasing the binding energy I_K and decreasing σ_K. The simplest way to correct for this effect [12] is to replace Z_{2K}^2 by $(Z_{2K} + Z_1)^2$, thus decreasing η_K in Eq. [1].

b. Polarisation [3]. At higher values v_1, the projectile may be thought of as passing outside the K-shell, deforming the wave function in such a way as to decrease I_K (since the electron is, on the average, farther away from the nucleus). This increases σ_K.

c. Relativity. Most calculations use (non-relativistic) hydrogenic wave functions. This cannot be correct for high-Z_2 targets (and even for medium Z_2 if the innermost part of the atom is probed by slow projectiles). Strongly bound electrons move fast; this increases T_m (due to the relativistic mass increase) and hence η_K. BRANDT and LAPICKI [13] have recently shown how this can be easily incorporated into the PWBA calculation.

d. Coulomb deflection. For low v_1, the projectile can no more be assumed to move at constant speed in a straight line. The Coulomb force both deflects the projectile and slows it down, thus decreasing η_K.

All these effects have been incorporated into the PWBA theory [3, 13]. The binding, relativity and Coulomb corrections are also contained in the formulation of the SCA theory given by LAEGSGAARD et al [12]. Because of the simple binding correction (see above), the latter is only good for small projectile velocities ($\xi < 0.25$).

Since the Coulomb correction is much different from unity wherever the relativity correction is [14] and since these two corrections tend to cancel each other, it is not easy to separate them by experiment.

There is, however, another theoretical approach which sheds light on the binding/polarization correction. FORD et al [15] have calculated K-shell ionization by protons using second order perturbation theory for cases where both relativity and Coulomb corrections are not important. Comparing their second order to their first order result should give the same binding/polari-

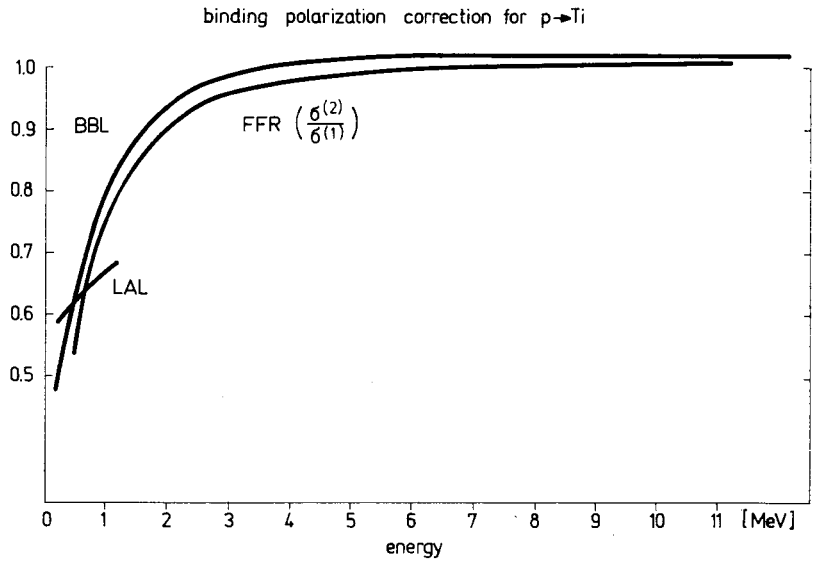

Fig. 1. The binding/polarization correction for protons on Ti according to three different theoretical approaches: BBL [3], FFR [15], and LAL [12]

zation correction as is obtained by comparing the corrected to the uncorrected PWBA cross section. Fig. 1 shows that there is indeed fairly good agreement between the two approaches. The SCA curve (labelled LAL) behaves quite differently, it is remarkable that it does not agree with the PWBA curve (labelled BBL) in the limit of vanishing energy (where it should be best).

4. Comparison of experimental and theoretical ionization cross-sections

Since the compilation of K-shell ionization cross sections was recently published by GARDNER and GRAY [16], we have been trying to use the large amount of information from Table I of that compilation to compare the experimental data both with each other and with the theories, using a computer program. First results have been presented before [17].

More recently, we have augmented the data base by new published data, and we have changed the program to normalize the data through division by the PWBA theory with all corrections. Ideally, then, all the normalized cross section data should be close to unity; in practice, we find almost all the data in the range (0.4, 1.6) and the great majority within (0.8, 1.2) i. e. the overall agreement with the corrected PWBA theory (for many different $Z_1 - Z_2$ combinations) is good, although some experiments may have excessive errors. By way of example, we present here a few representative graphs; the full comparison will be published elsewhere [20].

Fig. 2 shows relative cross sections for protons on Ne. The different symbols refer to different measurements identified by codes. Of this code, the first letter gives the type of measurement (X for X-ray, A or I for Auger); the second letter gives the type of target (G for gas, N for thin solids, K for a thick solid); the remaining symbols define the publication (see Table I). Before plotting, the experimental X-ray or Auger data have been converted to ionization cross sections using the table of fluorescence coefficients by KRAUSE [18]. Fig. 2 shows rather large discrepancies between different experiments at low energy.

Fig. 3 (p on Cu) shows good agreement between many different authors, and a few experimental discrepancies. Fig. 4 (p on Au) shows that the high energy points now agree rather well with the corrected PWBA theory, due to the inclusion of the relativity correction [13], but that the theory is too high for low energies. The corrected SCA theory is also plotted as a line ($\times - \times - \times$ in the region $\xi < 0.25$, and $+ - + - +$ in the region $\xi > 0.25$); it follows the data very well.

In Fig. 5, cross section data are plotted for protons ($E_1 \leq 15$ MeV) on five different targets ($_{47}\mathrm{Ag} - {}_{51}\mathrm{Sb}$), versus the reduced velocity variable ξ. Although the various corrections are not only functions of ξ, an approximately

universal behaviour is seen at low energy: the points bend down sharply at $\xi \approx 0.2$. The high points ($p \rightarrow {}_{49}In$) are due to KL76. Fig. 6 (p on Ag) shows that the low energy bend is found by three different groups: BR78, LA79, and BE79. This is somewhat in contradiction to BRANDT and LAPICKI [13] who state that only ANHOLT's data [14] are not in agreement with their theory. The reason for these different findings may be the somewhat different data base.

Table I

References for experimental data

AK74 R. AKSELSSON and T. B. JOHANSSON, Z. Physik, **266,** 245, 1974.
AN78 R. ANHOLT, Phys. Rev., **A17,** 983, 1978.
BE73 R. C. BEARSE, J. A. CLOSE, J. J. MALANIFY and C. J. Umbarger, Phys. Rev., **A7,** 126, 1973.
BE78 A. BERINDE, C. DEBERTH, I. NEAMU, C. PROTOP, N. SCINTEI, V. ZORAN, M. DOST, and S. RÖHL, J. Phys., **B11,** 2875, 1978.
BE79 O. BENKA and M. GERETSCHLÄGER, J. Phys. B. **13,** 3223, 1980.
BD78 T. BADICA, C. CIORTEA, A. PETROVICI and I. POPESCU, Rev. Roum. Phys., **23,** 1019, 1978.
BR78 C. BAUER, R. MANN and W. RUDOLPH, Z. Physik, **A287,** 27, 1978.
GR76A T. J. GRAY, P. RICHARD, R. L. KAUFFMAN, T. C. HOLLOWAY, R. K. GARDNER, G. M. LIGHT, J. GUERTIN, Phys. Rev., **A13,** 1344, 1976.
HO75A F. HOPKINS, R. BRENN, A. R. WHITTEMORE, J. KARP and S. K. BHATTACHERJEE, Phys. Rev., **A11,** 916, 1975.
HO75B F. HOPKINS, R. BRENN, A. R. WHITTEMORE, N. CUE and V. DUTKIEWICZ, Phys. Rev., **A11,** 1482, 1975.
KA77 M. KAMIYA. K. ISHII, K. SERA, S. MORITA and H. TAWARA, Phys. Rev., **A16,** 2295, 1977.
KB76 N. KOBAYASHI, N. MADEA, H. HORI and M. SAKAISAKA, J. Phys. Soc. Japan, **40,** 1421, 1976.
KH75 N. A. KHELIL and T. J. GRAY, Phys. Rev., **A11,** 893, 1975.
KL76 E. KOLTAY, D. BERENYI, I. KISS, S. RICZ, G. HOCK and J. BASCO, Z. Physik, **A278,** 299, 1976.
LA76 A. LANGENBERG and J. VAN ECK, J. Phys., **B9,** 2421, 1976.
LA79 E. LAEGSGAARD, E. U. ANDERSEN and F. HOGEDAL, Nucl. Instr. & Meth., **169,** 293, 1980.
LE75 R. LEAR and T. J. GRAY, Phys. Rev., **A8,** 2469, 1973.
LI73 R. B. LIEBERT, T. ZABEL, D. MILJANIC, H. LARSON, V. VALKOVIC and G. C. PHILLIPS, Phys. Rev., **A8,** 2336, 1973.
LO79B J. S. LOPES, A. P. JESUS and S. C. RAMOS, Nucl. Instr. & Meth., **169,** 311, 1980.
MD77A F. D. MCDANIEL, J. L. DUGGAN, P. D. MILLER and G. D. ALTON, Phys. Rev., **A15,** 846, 1977.
MI76 M. MILAZZO and G. RICCOBONO, Phys. Rev., **A13,** 578, 1976.
MK76 R. H. MCKNIGHT and R. G. RAINS, Phys. Rev., **A14,** 1388, 1976.
PE79 M. PONCET and Ch. ENGELMANN, Nucl. Instt. & Meth., **159,** 455, 1979.
RN76 R. R. RANDALL, J. A. BEDNAR, B. CURNUTTE and C. L. COCKE, Phys. Rev., **A13,** 204, 1976.
RS76 MD. RASHIDUZZAMAN KHAN, D. CRUMPTON and P. E. FRANCOIS, J. Phys., **B9,** 455, 1976.
SO76 C. G. SOARES, R. D. LEAR, J. T. SANDERS and H. A. VAN RINSVELT, Phys. Rev., **A13,** 953, 1976.
ST75 N. STOLTERFOHT and D. SCHNEIDER, Phys. Rev., **A11,** 721, 1975.
TR77 J. TRICOMI et al, Phys. Rev., **A15,** 2269, 1977.
WL76 S. R. WILSON, F. D. MCDANIEL, J. R. ROWE and J. L. DUGGAN, Phys. Rev., **A16,** 903, 1977.
WO74 C. W. WOODS, R. L. KAUFFMAN, K. A. JAMISON, C. L. COCKE and P. RICHARD, J. Phys. **B7,** L474, 1974.
WO76 C. W. WOODS, R. L. KAUFFMAN, K. A. JAMISON, N. STOLTERFOHT and P. RICHARD, Phys. Rev., **A13,** 1358, 1976.

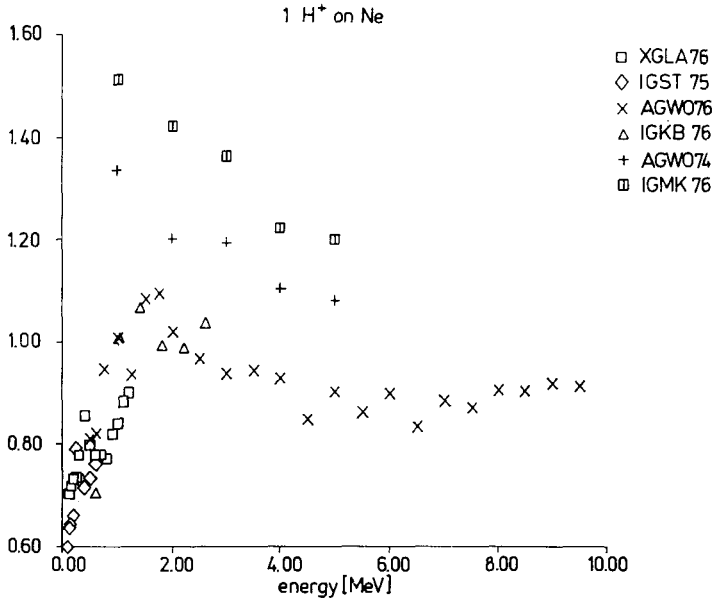

Fig. 2. Experimental K-shell ionization cross section for protons on Ne versus projectile energy, divided by the fully corrected PWBA theory [3, 13]. The different symbols correspond to different references (see Table I), the first two letters define the type of measurement and the type of target (see text)

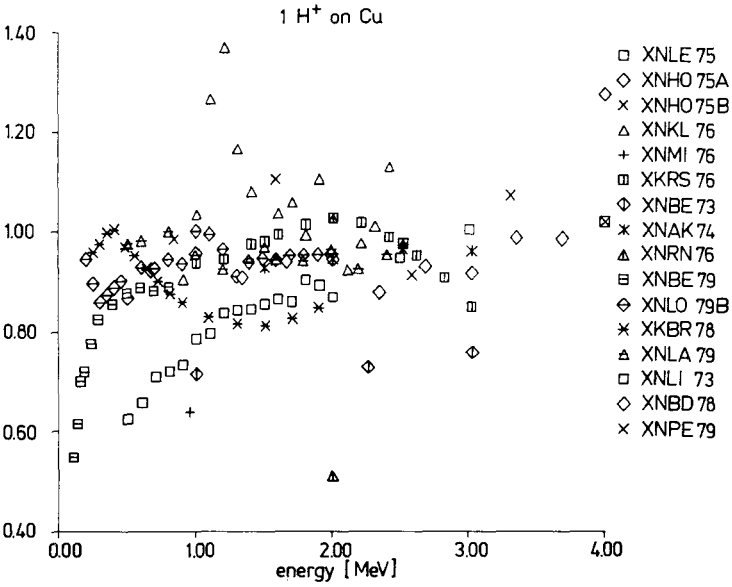

Fig. 3. Like Fig. 2, for protons on Cu. Note that a few symbols have been used twice

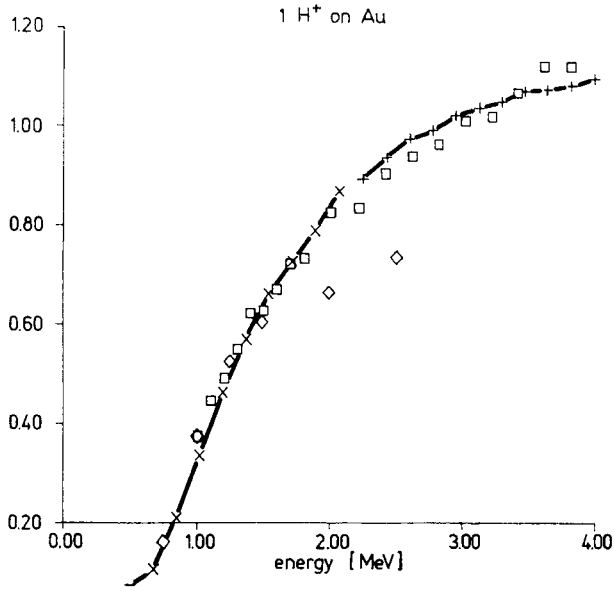

Fig. 4. Like Fig. 2, for protons on Au. The (normalized) SCA-theory [12] is plotted here as a line (x–x–x for $1 > 0.25$, +—+—+ for $\xi > 0.25$). It fits the data at low energies much better than the PWBA theory. Data are due to KA77 (squares) and AN78 (diamonds)

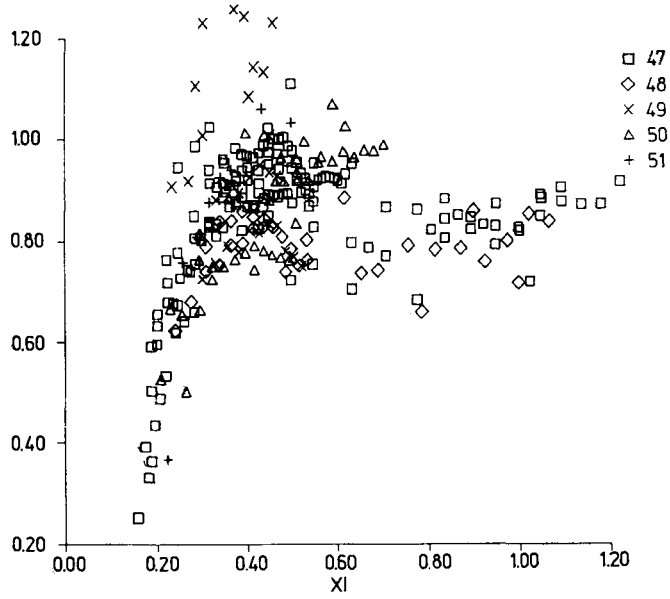

Fig. 5. Experimental K-shell ionization cross sections, normalized as in Fig. 2, plotted versus the reduced velocity ξ (Eq. 3), for protons on Ag, Cd, In, Sn, and Sb. The different symbols correspond to different target atomic numbers, as shown. Note the low energy bend at $\xi \sim 0.2$

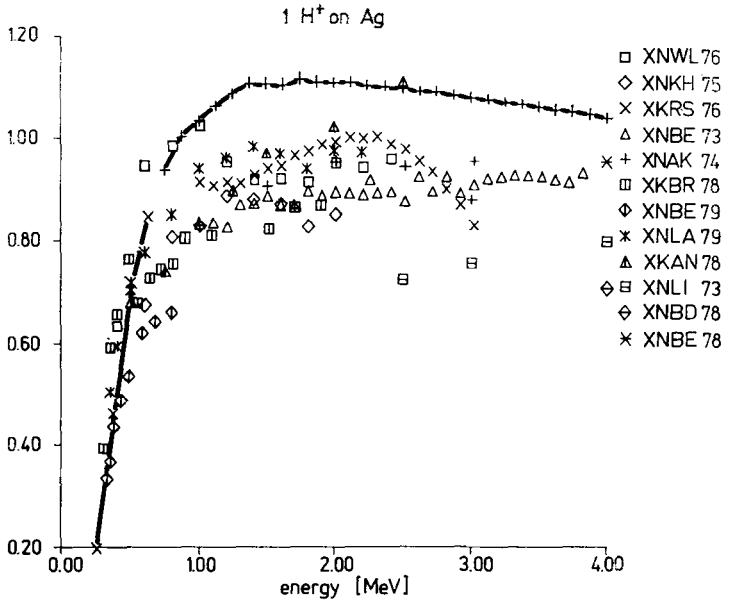

Fig. 6. Like Fig. 4, for protons on Ag

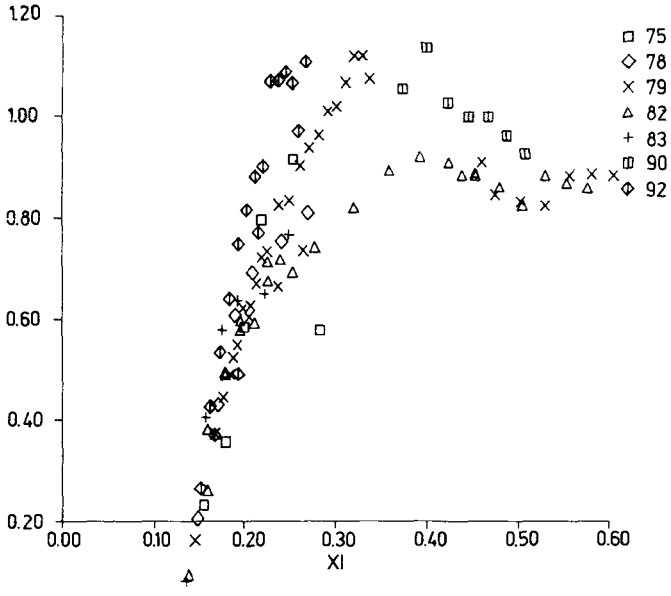

Fig. 7. Like Fig. 5, for protons on heavy targets

Fig. 7 (protons on heavy targets: $_{75}$Re — $_{92}$U, $E_1 < 13$ MeV) shows the same general behaviour. The low energy bend is again found by three groups: KA77, AN78, and LA79.

Fig. 8 (alphas on targets from $_{22}$Ti to $_{30}$Zn, $E_1 < 10$ MeV) shows very many points within (0.8, 1.2), a few high points (KL76) and a few low points (SO76). Here, the bend at $\xi \sim 0.2$ is only based on measurements by one group (BE79).

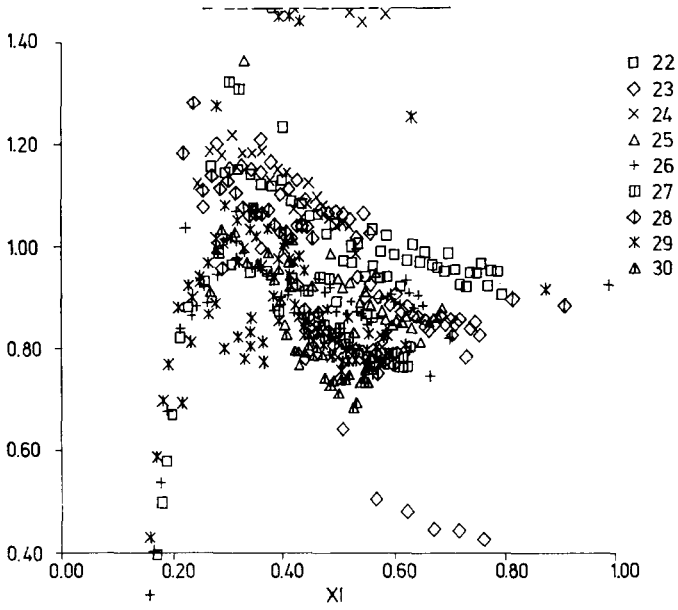

Fig. 8. Like Fig. 5, for alphas on targets from Ti to Zn

There may also be an indication of a maximum at $\xi \sim 0.3$. Fig. 9 (alphas on heavy targets, $E_1 < 60$ MeV) shows the same general behaviour; the low energy points are here only due to AN78.

The remaining figures refer to slightly heavier projectiles. Figs. 10 and 11 (^{14}N projectiles on targets from $_{20}$Ca to $_{51}$Sb, $E < 36$ MeV) show a new feature: a pronounced minimum at $\xi \sim 0.6$. Whereas Fig. 10 contains almost only data by MD77A, Fig. 11 has data by four different groups: MD77A, BR78, GR76A, TR77.

Fig. 12 (^{16}O on $_{26}$Fe to $_{35}$Br, $E < 91$ MeV) shows the same minimum less clearly due to the somewhat discrepant data. Fig 13 (^{16}O on $_{37}$Rb to $_{62}$Sm, $E < 56$ MeV) may again show the maximum at $\xi \sim 0.3$, though not very clearly. Fig. 14 (^{16}O on $_{67}$Ho to $_{92}$U, $E < 56$ MeV) shows the bend at $\xi \sim 0.2$ and the maximum at $\xi \sim 0.3$.

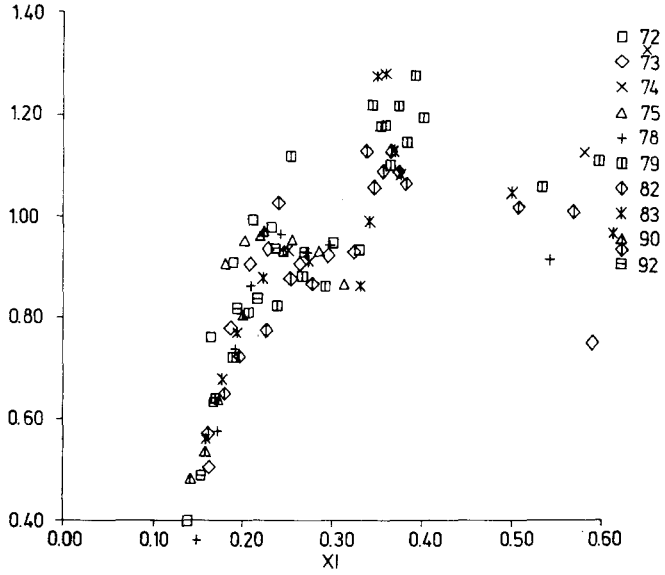

Fig. 9. Like Fig. 5, for alphas on heavy targets

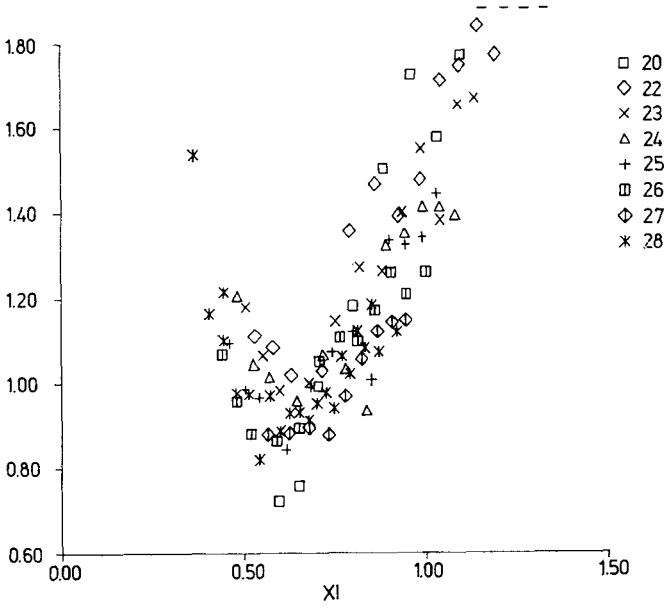

Fig. 10. Like Fig. 5, for ^{14}N projectiles on targets from Ca to Ni. Note the minimum at $\xi \sim 0.6$

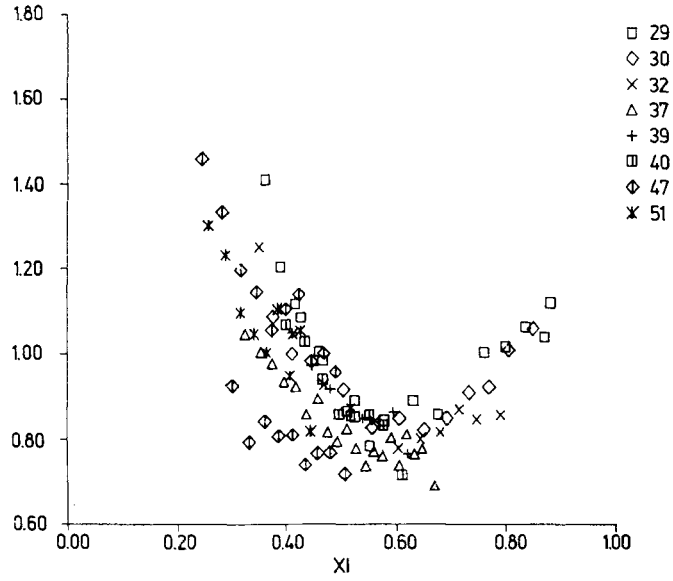

Fig. 11. Like Fig. 5, for ^{14}N projectiles on targets from Cu to Sb

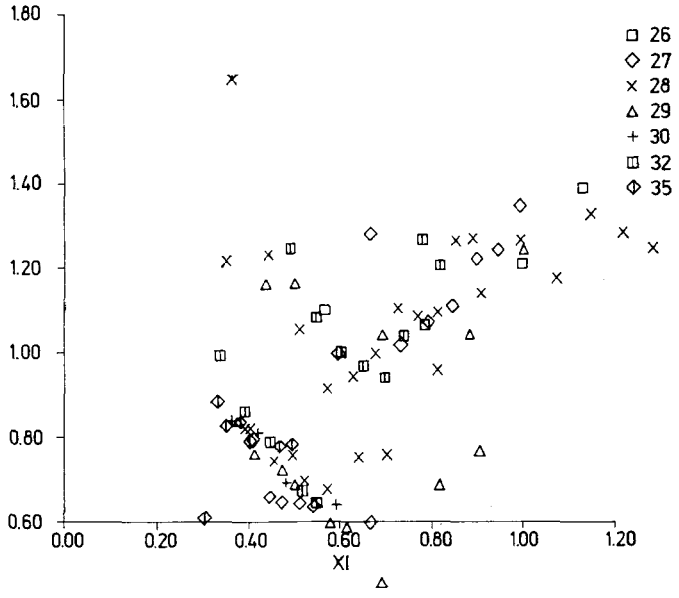

Fig. 12. Like Fig. 5, for ^{16}O projectiles on targets from Fe to Br. A possible minimum at $\xi \sim 0.6$ is barely perceptible due to somewhat discrepant data

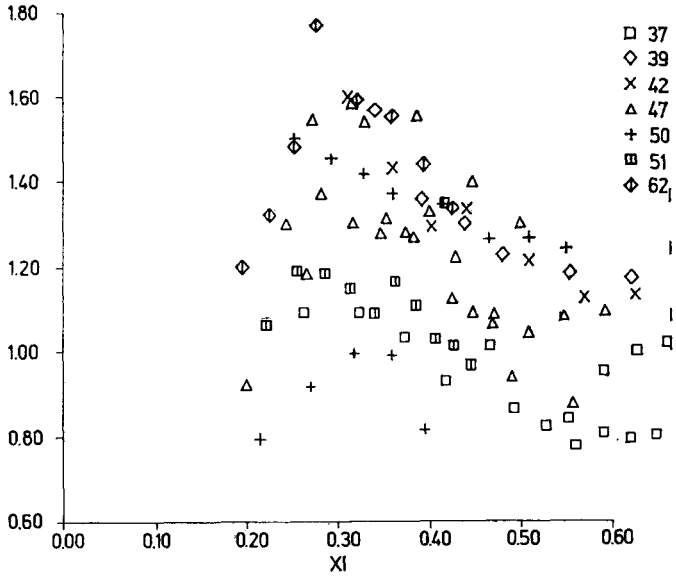

Fig. 13. Like Fig. 5, for ^{16}O projectiles on targets from Rb to Sm

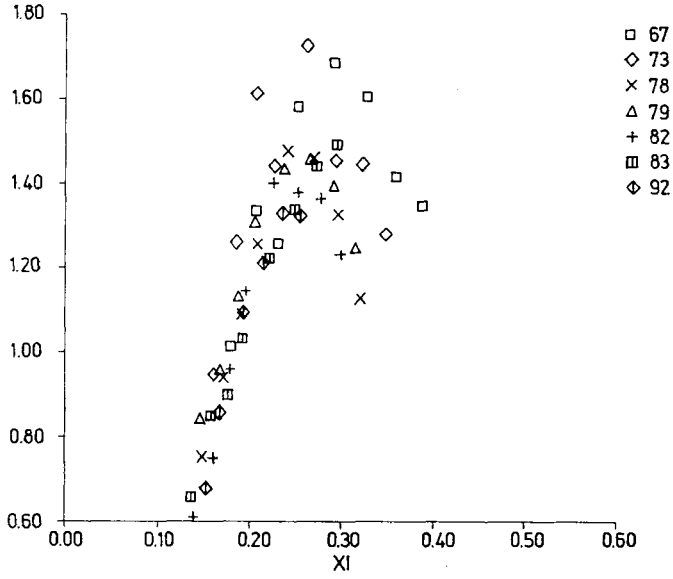

Fig. 14. Like Fig. 5, for ^{16}O projectiles on targets from Ho to U. Note the maximum at $\xi \sim 0.3$

In retrospect, it can be noted that not only the bend at $\xi \sim 0.2$ but also the features at $\xi \sim 0.3$ and $\xi \sim 0.6$ can be seen (or guessed) from the Figures for protons and alphas, but that they are less pronounced there than for the heavier projectiles.

5. Discussion

Although these remaining discrepancies between the corrected PWBA theory due to BRANDT et al [3, 13] and experiments are not very large, it would be interesting to find reasons. Clearly, this will not be possible from our comparisons alone, but will require theoretical insight also.

Concerning the bend at $\xi \sim 0.2$, we may assume, following the work of KOCBACH [19] and ANHOLT [14], that BRANDT's [3, 13] Coulomb correction factor is not as different from unity as it should be.

Since electron capture by the projectile is not included in the theories used, the question arises whether the maximum at $\xi \sim 0.3$ could be due to this effect. Taking ^{16}O projectiles as an example, one would indeed expect the maximum of K-capture to occur around $E_1 = 26$ MeV (where v_1 equals the velocity of projectile K-electrons). But the corresponding values of ξ would then lie between $\xi = 0.17$ (for U) and $\xi = 0.53$ (for Rb), whereas the maximum is empirically found at a fixed value ξ.

Finally, one may ask whether the features at $\xi = 0.3$ and 0.6 are due to not quite satisfactory theoretical corrections. Here the binding correction would be the most likely candidate since it becomes more important with increasing Z_1. For ^{14}N projectiles, e. g. it amounts to about 0.16 for $\xi = 0.6$, whereas the other corrections are close to unity. Hence, the deviations may well be due to the binding correction.

The corrected SCA theory is not within its range of validity ($\xi < 0.25$) on most graphs. Where it is valid, however, it follows the data better than the PWBA theory.

6. Acknowledgements

I should like to thank Prof. BASBAS, DUGGAN and MCDANIEL for their interest and help that made it possible for me to produce the figures by means of a computer program written during several stays at North Texas State University. The help of Prof. MACKEY, who wrote the Plot Package program, was also essential. Finally, this work would have been impossible without the help of Prof. GRAY who provided me his tables in the form of punched cards.

REFERENCES

1. H. H. ANDERSEN and J. F. ZIEGLER, Hydrogen Stopping Powers and Ranges in all Elements, Pergamon Press, New York, 1977.
2. E. MERZBACHER and H. W. LEWIS, in: Encyclopedia of Physics, S. Flügge, ed. Springer, Berlin, **34**, 166 ff, 1958.

3. G. BASBAS, W. BRANDT and LAUBERT, Phys. Rev., **A17**, 1655, 1978.
4. Intern. Conf. on Particle induced X-ray Emission and its Analytical Applications, Lund (Sweden) 1976; Nucl. Instr. & Meth. 142, 1977.
5. 1978 Conf. Appl. small Accelerators in Res. and Ind., Denton TX, 1978; IEEE Trans. Nucl. Sc. NS-26, No. 1, part 2, 1979.
6. O. BENKA, M. GERETSCHLÄGER and A. KROPF, Nucl. Instr. & Meth., **149**, 441, 1978.
7. J. VEGH et al, Nucl. Instr. & Meth., **153**, 553, 1978.
8. S. A. E. JOHANSSON and T. B. JOHANSSON, Nucl. Instr. & Meth., **137**, 473, 1976.
9. J. M. HANSTEEN, in: Adv. Atomic and Molec. Phys., ed. by D. R. Bates and B. Bederson, Acad. Press, New York, **11**, 299 ff. 1975.
10. D. H. MADISON and E. MERZBACHER, in: Atomic Inner Shell Processes, ed. by B. Crasemann, Academic Press, New York, 1975, Vol. 1,1.
11. G. BASBAS, Proc. 4th Conf. Sci. and Ind. Appl. of Small Accelerators, Denton TX, 1976; IEEE, New York, 1977, 142.
12. E. LAEGSGAARD, J. U. ANDERSEN and M. LUND, in: 10th Int. Conf. Phys. Electronic Atomic Coll. (Paris), G. Watel, ed., North-Holland Publ. Co., Amsterdam, 1978, p. 353.
13. W. BRANDT and G. LAPICKI, Phys. Rev., **A20**, 465, 1979.
14. R. ANHOLT, Phys. Rev., **A17**, 983, 1978.
15. A. L. FORD, E. FITCHARD and J. F. READING, Phys. Rev., **A16**, 133, 1977.
16. R. K. GARDNER and T. J. GRAY, At. Data Nucl. Data Tables **21**, 515, 1978.
17. H. PAUL, Nucl. Instr. & Meth., **169**, 249, 1980.
18. M. O. KRAUSE, J. Phys. Chem. Ref. Data **8**, 307, 1979.
19. L. KOCBACH, Phys. Norv., **8**, 187, 1976.
20. H. PAUL, At. Data Nucl. Data Tables, in print.